JOC The Journal of Organic Chemistry

Article

pubs.acs.org/joc

Synthesis and Properties of Fluorescence Dyes: Tetracyclic Pyrazolo[3,4-*b*]Pyridine-Based Coumarin Chromophores with Intramolecular Charge Transfer Character

Jianhong Chen,[†,‡,§] Weimin Liu,[†,§] Jingjin Ma,[†,‡] Haitao Xu,[†] Jiasheng Wu,[†] Xianglin Tang,[†,‡] Zhiyuan Fan,[†,‡] and Pengfei Wang*[,†]

[†]Key Laboratory of Photochemical Conversion and Optoelectronic Materials, Technical Institute of Physics and Chemistry, Chinese Academy of Sciences, Beijing, 100190, China

[‡]Graduate School of Chinese Academy of Sciences, Beijing, 100049, China

Supporting Information

ABSTRACT: Two series of new tetracyclic pyrazolo[3,4-*b*]pyridine-based coumarin chromophores were synthesized through a facile reaction between 3-aldehyde-7-diethylaminocoumarin (**5**) or 3-acetyl-7-diethylaminocoumarin (**6**) and 5-aminopyrazole derivatives (**7**) in a one-pot procedure. Different condensed products were obtained from compounds **5** and **6**, and the potential reaction mechanism was studied using the reaction of **5** with 5-amino-1-phenylpyrazole (**7a**). The molecular structures were characterized by NMR and HRMS and confirmed by X-ray diffraction. The photophysical, electrochemical, and thermal properties of these compounds were investigated by absorption spectroscopy, fluorescence spectroscopy, single photon counting technique, cyclic voltammetry, thermogravimetric analysis, etc. Results show that the compounds exhibited high fluorescence quantum yields and good electrochemical, thermal, and photochemical stabilities. In addition, the application of these highly fluorescent compounds in living cell imaging was also explored by laser scanning confocal microscopy.

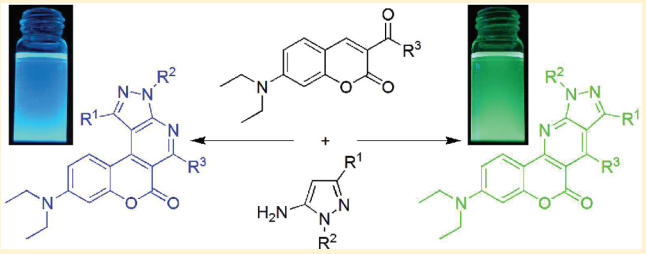

INTRODUCTION

The design and synthesis of brightly emissive molecules with a polycyclic aromatic backbone remain key objectives of current research in view of their potential applications in optoelectronic devices[1] and sensing materials.[2] From the perspective of molecular design for highly fluorescent dyes, an important approach is to design fused heterocyclic aromatic analogues with intramolecular charge transfer (ICT) character because of the following advantages: (i) the suppression of both the proximity effect caused by the interaction of n−π and π−π electron configurations and internal conversion decay from the free rotation of unbridged double bonds; (ii) minimal self-reabsorption, especially in the solid state; and (iii) relatively narrow emission bands resulting from reduced vibration.[3]

Pyrazolo[3,4-*b*]pyridine derivatives as aza analogues of indazole have received considerable attention given their significant biological activities.[4] Their fused large conjugated derivatives are highly fluorescent and used in organic light-emitting diodes (OLEDs) or as chemosensors, such as pyrazolo[3,4-*b*]quinoxaline,[3] pyrazoloquinoline,[5] and bipyrazolopyridine.[6] Coumarin derivatives with ICT character have been widely investigated and applied in diverse fields, including biomedicine,[7] OLEDs,[8] chemosensors,[9] and laser dyes.[10] It can be conceived that compounds containing pyrazolo[3,4-*b*]-pyridine and coumarin moieties may show extraordinary properties. In the present work, two series of tetracyclic pyrazolo[3,4-*b*]pyridine-based coumarin (PPC) derivatives, which show distinct photophysical properties because of their different molecular skeletons, were designed and synthesized. Interestingly, two types of tetracyclic PPC derivatives can be derived in a one-pot procedure; this approach is highly attractive in synthetic chemistry similar to domino reactions.[11] The readily available pyrazolo[3,4-*b*]pyridine and coumarin-fused scaffold may serve as a new opportunity for the development of novel pyrazolo[3,4-*b*]pyridine/coumarin-based organic functional materials. The properties of these tetracyclic PPC derivatives were also investigated by X-ray diffraction, absorption spectroscopy, fluorescence spectroscopy, single photon counting technique, cyclic voltammetry, thermogravimetric analysis, and density functional theory (DFT) calculations. As a straightforward application, tetracyclic PPC derivatives (**1a** and **2a**) were also used for confocal fluorescence imaging in living HeLa cells.

RESULTS AND DISCUSSION

Synthesis and Mechanism. Compounds **5** and **6** were synthesized according to previously reported procedures.[12]

Received: February 7, 2012
Published: March 19, 2012

   dx.doi.org/10.1021/jo3002722 | *J. Org. Chem.* 2012, 77, 3475−3482

Table 1. Synthesis of Tetracyclic PPC Derivatives

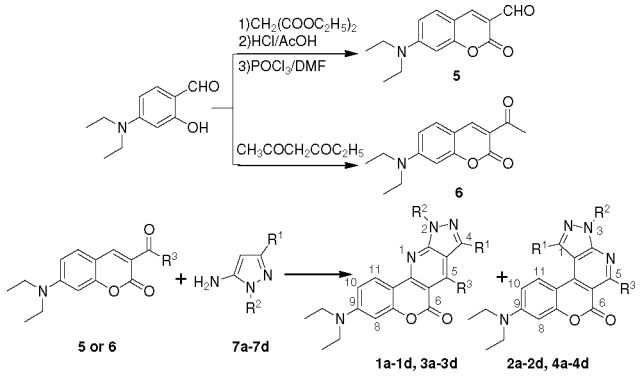

entry	R^1	R^2	R^3	yield	
5 + **7a**	H	Ph	H	**1a** (50%)	**2a** (23%)
5 + **7b**	CH_3	Ph	H	**1b** (69%)	**2b** (1%)
5 + **7c**	Ph	Ph	H	**1c** (75%)	**2c** (trace)
5 + **7d**	Ph	CH_3	H	**1d** (76%)	**2d** (trace)
6 + **7a**	H	Ph	CH_3	**3a** (trace)	**4a** (19%)
6 + **7b**	CH_3	Ph	CH_3	**3b** (trace)	**4b** (23%)
6 + **7c**	Ph	Ph	CH_3	**3c** (trace)	**4c** (17%)
6 + **7d**	Ph	CH_3	CH_3	**3d** (trace)	**4d** (22%)

Scheme 1. Proposed Reaction Pathways

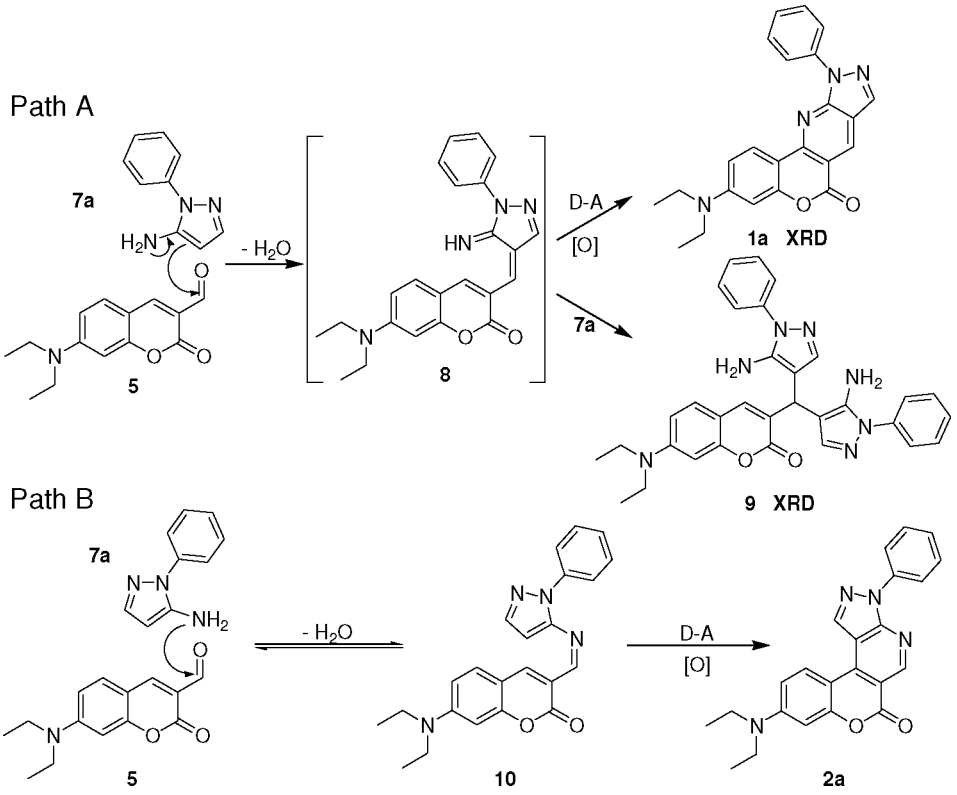

Tetracyclic PPC derivatives (**1a**−**1d**, **2a** and **2b**, and **4a**−**4d**) were obtained in a one-pot procedure through the condensation of **5** or **6** with corresponding 5-aminopyrazole derivatives (**7a**−**7d**) in ethanol without any catalyst (Table 1). Interestingly, different primary products were obtained from compounds **5** and **6**.

We chose the reaction of compounds **5** and **7a** to study the potential reaction mechanism, as shown in Scheme 1. The reactions may proceed via two different reaction procedures including C−C or C−N condensation reaction, intramolecular Diels−Alder reaction, and aromatization. In path A, the addition of the 4-C atom of **7a** to **5** formed unstable intermediate **8**, which can be converted into main product **1a**.[13] The existence of intermediate **8** can also be confirmed by byproduct **9** (yield 8%), which may be obtained through the addition of another molecular **7a** to intermediate **8** and confirmed by X-ray crystallography (Figure S8 in Supporting Information). Likewise, in path B, compound **2a** was obtained

dx.doi.org/10.1021/jo3002722 | J. Org. Chem. 2012, 77, 3475−3482

by the C−N condensation reaction of **5** and **7a**, accompanied by the formation of a key intermediate **10** (yield 5%). Schiff base **10** was separated, and **2a** was also obtained through the reflux of sole **10** under the same conditions.[4a] These results are supported by the findings derived from X-ray diffraction, ^{1}H NMR, ^{13}C NMR, and HRMS.

The main products obtained from compound **5** are C−C condensation products (**1a**−**1d**); the derivation can be explained by the theoretical calculations. For example, the difference in relative energy between **1a** and **2a** was about −7.6 kcal/mol, with preference for the formation of **1a** as the major thermodynamically favored product.[14] Moreover, the yields of C−N condensation products (**2a**−**2d**) for **5** decreased rapidly in the series hydrogen → methyl → phenyl, in line with the increasing steric hindrance of the 3-C atom of 5-aminopyrazole derivatives: 23% for **2a**, 1% for **2b**, and trace for **2c** and **2d** (Table 1). By contrast, the C−N condensation compounds (**4a**−**4d**) were the primary products for compound **6** through a path similar to path B because the reactivity of carbonyl decreased rapidly given the steric hindrance of methyl. Compound **6** is highly difficult to react through a path similar to path A (trace for **3a**−**3d**).

X-ray Structures and NMR Spectra. The molecular structures of **1a**, **1b**, **2b**, and **4a**−**4d** were elucidated by X-ray crystallography (Figures 1 and S1−S7), revealing pyrazolo[3,4-*b*]pyridine and coumarin-fused skeleton (see Supporting Information for details). They are all racemic mixtures given the helix structure and the presence of both enantiomers in the unit cells. The tetracyclic molecular skeletons are twisty because of steric hindrance. The torsion angles θ of the M isomers for **1a** (C(12)−C(13)−N(1)−N(3)), **1b** (C(19)−C(20)−N(1)−N(2)), **2b** (C(17)−C(16)−N(2)−N(1)), **4a** (C(5)−C(10)−N(4)−N(3)), **4b** (C(20)−C(21)−N(2)−N(1)), **4c** (C(5)−C(6)−N(4)−N(3)), and **4d** (C(8)−C(7)−N(1)−N(2)) (for atomic labels, see Figures 1 and S1−S7) are listed in Table 2. Two torsion angles were observed in the antiparallel crystal packing of **1a** and **4a**; thus, they have more isomers in the unit cells than the other compounds. Compound **1b** showed more planar and more π-conjugate interaction than compounds **2b** and **4b**−**4d**. The torsion angle of **4b** is larger than that of **2b** because of an additional methyl. Because of the steric hindrance of the substituent on the 3-C atom of pyrazole, the torsion angles of **4b** and **4c** are larger than that of **4a**. These conclusions are consistent with the results of the DFT calculations. Details of the X-ray experimental conditions, cell data, and refinement data of compounds **1a**, **1b**, **2b**, and **4a**−**4d** are summarized in Table 3.

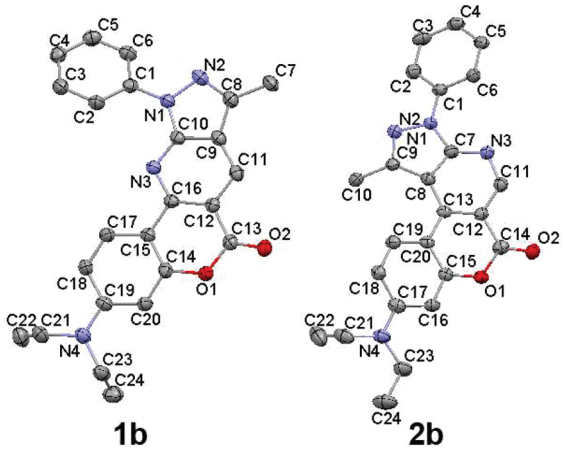

Figure 1. Crystal structures of **1b** and **2b** with ellipsoids shown at the 50% probability level (hydrogen atoms are omitted for clarity).

Table 2. Crystallographic and Theoretical Calculation Data of 1a, 1b, 2b and 4a−4d

product	θ^a(deg)	θ^b(deg)
1a	7.70/2.55	2.52
1b	2.83	2.49
2b	18.54	19.14
4a	11.87/0.16	5.50
4b	22.04	22.42
4c	16.78	26.33
4d	15.43	25.19

[a]The torsion angle determined from crystal structure. [b]The torsion angle determined from theoretical calculation.

Furthermore, because of the anisotropic effects of the phenyl, H_a and H_b (for atomic labels, see Figure 2) of **4c** and **4d** exhibited distinct upfield shifts[15] (about 0.78 and 0.82 ppm for H_a, 1.13 and 1.15 ppm for H_b, respectively) compared with **4a** in ^{1}H NMR, while H_c slightly changed (6.59, 6.53, and 6.48 ppm for **4a**, **4c**, and **4d**, respectively). Moreover, because H_b is closer to phenyl than H_a, the change in chemical shift of H_b is greater (1.13 ppm vs 0.78 ppm for **4c**).

Photophysics. The absorption and fluorescence spectra of all of the compounds were investigated in different solvents (Figures 3, S9, and S10). The C−N condensation products (**2a**, **2b**, and **4a**−**4d**) exhibited a narrow absorption band, whereas the C−C condensation products (**1a**−**1d**) displayed a broad band with a shoulder peak (an ICT transition[16]) at lower energy. Compared with the C−C condensation products, those of the C−N condensation products exhibited a slight red shift for absorption peaks because the decrease in π-conjugate interaction for it elevates the HOMO level, thereby resulting in a narrow band gap. In cyclohexane, the structured absorption bands indicate that a narrow distribution of vibrational states is involved in the electronic transition.[17] For all of the compounds, the maximum absorption band is attributed to the $\pi \rightarrow \pi^*$ transition because of their high molar extinction coefficients of above 10^4 M^{-1} cm^{-1} in CH_2Cl_2 (Table 4).[18] Although solvent polarity has little effect on the absorption spectra, significant bathochromic shift of the emission bands was observed with increasing solvent polarity because of the ICT character. These results suggest that the excited states possess more polar character than the ground states.[19] Figure 3 shows that the fluorescence for **1b** and **2b** had two different origins: a locally excited (LE) state responsible for a $\pi^* \rightarrow \pi$ fluorescence and an ICT state, which produces ICT emission.[20] In the polar solvents, the LE emission vanished, and only ICT emission was observed. The emission spectra of **1b** and **2b** became red-shifted and broadened as solvent polarity increased from cyclohexane to CH_3OH, which is typical of ICT excited states.[21] It indicates effective electronic communication between the diethylamino group and the pyrazolopyridine core, which is compatible with the result of the DFT calculations.[22] Given the stronger ICT properties, the C−C condensation products exhibited longer fluorescence lifetimes and larger Stokes shifts in CH_2Cl_2 than the C−N condensation products (Table 4). The magnitude of Stokes shifts for the C−C condensation products implies a large difference between the

dx.doi.org/10.1021/jo3002722 | J. Org. Chem. 2012, 77, 3475−3482

Table 3. Selected Crystallographic Data of 1a, 1b, 2b and 4a−4d

	1a	1b	2b	4a	4b	4c	4d
formula	$C_{23}H_{20}N_4O_2$	$C_{24}H_{22}N_4O_2$	$C_{24}H_{22}N_4O_2$	$C_{24}H_{22}N_4O_2$	$C_{25}H_{24}N_4O_2$	$C_{30}H_{26}N_4O_2$	$C_{25}H_{24}N_4O_2$
formula weight	384.43	398.46	398.46	398.46	412.48	474.55	412.48
crystal system	triclinic	monoclinic	triclinic	monoclinic	triclinic	triclinic	triclinic
space group	$P\bar{1}$	$P2_1/c$	$P\bar{1}$	$P2_1/c$	$P\bar{1}$	$P\bar{1}$	$P\bar{1}$
a, Å	9.4170(18)	6.4584(13)	7.486(2)	12.609(4)	9.372(3)	10.157(3)	9.573(4)
b, Å	12.514(3)	20.649(4)	11.283(3)	15.739(3)	11.126(4)	10.670(3)	9.815(4)
c, Å	16.573(4)	15.101(3)	12.414(4)	19.556(4)	11.340(4)	11.257(3)	11.061(4)
α, deg	88.219(10)	90.00	80.3410(18)	90.00	105.318(4)	103.417(8)	92.907(7)
β, deg	75.860(10)	101.92(3)	76.4090(14)	93.380(3)	105.023(4)	93.162(6)	95.692(7)
γ, deg	80.763(10)	90.00	73.2770(15)	90.00	104.512(2)	90.024(5)	94.927(7)
V, Å^3	1869.24	1970.44	970.41	3874.2	1034.84	1184.77	1028.49
Z	4	4	2	8	2	2	2
ρ, g/cm^3	1.366	1.343	1.364	1.366	1.324	1.33	1.332
R factor (%)	6.33	7.85	7.61	8.14	6.57	7.56	6.87
number of reflections	21183	17579	7297	28790	13801	13324	7745
R_{int}	0.0819	0.0635	0.0501	0.0807	0.0466	0.0552	0.0475
$R(F)$ (all data)	0.0873	0.1003	0.0955	0.0952	0.0772	0.0947	0.0917
$wR(F^2)$ (all data)	0.1458	0.1435	0.1616	0.1784	0.1396	0.1475	0.1684

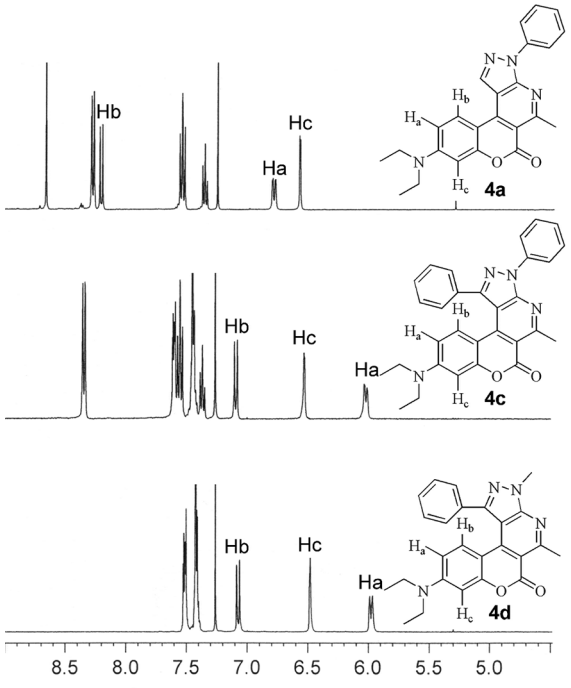

Figure 2. Partial ^{1}H NMR spectra of compounds **4a**, **4c**, and **4d**.

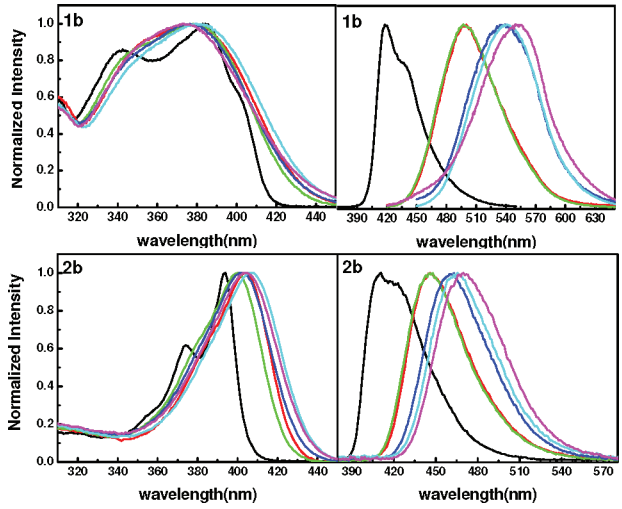

Figure 3. Absorption (left) and fluorescence spectra (right) of compounds **1b** and **2b** in different solvents ($c = 1 \times 10^{-5}$ M): black (cyclohexane), red (CH_2Cl_2), green (ethyl acetate, EA), blue (CH_3CN), cyan (DMF), and magenta (CH_3OH).

excited state reached after absorption and that from which the emission starts.[19]

The fluorescence quantum yields (Φ) of all of the compounds are given in Table 5. Compounds **1a−1d** exhibited low Φ in polar solvents because of the strong ICT character.[23] A general trend is that the C−C condensation products showed lower Φ compared with the C−N condensation products (comparison between **1a** and **2a**, and **1b** and **2b**). The addition of a substituent decreased Φ from 0.717 to 0.310, in comparison with the results obtained for **1a**, **1b**, and **1c** in cyclohexane. This decrease is presumably due to an increase in the nonradiative decay pathways caused by C−C bond vibrations.[21] The C−N condensation products (**2a**, **2b**, and **4a−4d**) showed intense blue fluorescence even in strong polar solvents (0.222 to 0.430 in CH_3OH). All of the compounds displayed a positive solvent effect and high fluorescence quantum yields both in less polar solvents and in the solid state. Compounds **2a** and **2b** displayed two distinct emission

Table 4. Photophysical Properties of All Compounds in CH_2Cl_2

product	λ_{max} (nm)	λ_{em} (nm)	Stokes	ε (M^{-1} cm^{-1})	τ (ns)
1a	379	501	6425	25500	16.85
1b	377	499	6485	30200	17.06
1c	359	509	8209	45300	17.86
1d	350	506	8809	36500	18.91
2a	405	441	2016	62000	2.48
2b	404	445	2281	25000	3.34
4a	403	439	2035	53000	2.72
4b	403	452	2690	37100	3.61
4c	410	461	2698	46200	3.51
4d	408	461	2818	38200	4.28

dx.doi.org/10.1021/jo3002722 | J. Org. Chem. 2012, 77, 3475−3482

Table 5. Fluorescence Quantum Yields of All Compounds in Different Solvents and the Solid State

product	Φ (cyclohexane)	Φ (CH_2Cl_2)	Φ (EA)	Φ (CH_3CN)	Φ (DMF)	Φ (CH_3OH)	Φ(λ_f) (solid state)
1a	0.717	0.325	0.233	0.023	0.023	0.002	0.42 (479)
1b	0.486	0.312	0.231	0.030	0.030	0.002	0.58 (478)
1c	0.310	0.240	0.195	0.018	0.013	0.002	0.33 (470)
1d	0.338	0.292	0.202	0.020	0.015	0.002	0.62 (486)
2a	0.926	0.916	0.885	0.554	0.296	0.222	0.44 (474, 501)
2b	0.694	0.688	0.601	0.445	0.370	0.279	0.50 (486, 564)
4a	0.931	0.829	0.685	0.627	0.37	0.294	0.48 (456)
4b	0.852	0.827	0.733	0.608	0.562	0.428	0.60 (476)
4c	0.635	0.653	0.634	0.51	0.51	0.396	0.09 (473)
4d	0.699	0.673	0.627	0.493	0.483	0.430	0.44 (470)

peaks in the solid state, which may be due to the existence of intermolecular interactions.[24] Compounds **1c** and **4c** exhibited weak emission in the solid state compared with the other compounds probably because of well-ordered π stacking that led to strong intermolecular interactions and fluorescence self-quenching.[25]

Electrochemical and Thermal Properties. All of the compounds displayed a one-electron reversible oxidation wave (Figure S11). As shown in Table 6, the oxidation processes

Table 6. Electrochemical and Thermal Data of the Dyes

product	E_{ox}[a] (V)	HOMO[b] (eV)	LUMO[c] (eV)	ΔE_{op}[d] (eV)	T_g[e] (°C)	T_m[f] (°C)	T_d[g] (°C)
1a	0.69	5.49	2.66	2.83	68	198	351
1b	0.68	5.48	2.62	2.86	69	218	316
1c	0.69	5.49	2.74	2.75	87	221	358
1d	0.68	5.48	2.67	2.81	77	217	320
2a	0.79	5.59	2.72	2.87	60	222	287
2b	0.77	5.57	2.69	2.88	60	203	314
4a	0.77	5.57	2.70	2.87	72	235	317
4b	0.74	5.54	2.66	2.88	58	217	325
4c	0.74	5.54	2.74	2.80	73	242	310
4d	0.73	5.53	2.69	2.84	71	218	298

[a]Obtained from cyclic voltammograms. [b]Derived from the oxidation potential using $E_{HOMO} = 4.8 + E_{ox}$. [c]Deduced using the formula $E_{LUMO} = E_{HOMO} - \Delta E_{op}$. [d]Calculated from the optical edge measured in CH_3CN. [e]Glass transition temperature. [f]Melting point temperature. [g]Decomposition temperature.

occurred at slightly more positive potentials for **2a**, **2b**, and **4a**−**4d** (0.73−0.79 V) relative to those of **1a**−**1d** (0.68−0.69 V). The causes of the anodic shift for **2a**, **2b**, and **4a**−**4d** may be their efficient ICT character.[26] The HOMOs (5.48−5.59 eV) and LUMOs (2.62−2.74 eV) of all of the compounds are well matched with those of the most commonly used hole transport material α-naphthylphenylbiphenyl diamine (NPB, 5.50 eV)[27] and electron transport material 1,3,5-tris(*N*-phenylbenzimidazol-2-yl)benzene (TPBI, 2.7 eV),[28] respectively, suggesting their potential applications as emitters in OLEDs. The thermal behavior of all of the materials was determined through a repeated heating−cooling cycle by differential scanning calorimetry (Table 6). All of the compounds exhibited moderate glass transition temperatures (T_g) varying from 58 to 87 °C, and thermal decomposition (T_d) ranged from 287 to 358 °C.

Theoretical Basis. To investigate the geometric and electronic properties of all of the compounds, quantum calculations using the Gaussian 03 program have been performed.[29] The calculations were optimized using the restricted B3LYP/6-31 G (d) functions at the DFT level. The calculated typical torsion angles of compounds **1a**, **1b**, **2b**, and **4a**−**4d** are listed in Table 2. As expected, the result of geometry optimizations is consistent with the experimental data obtained from single-crystal structures. For **1b**, the calculated angle (2.49°) well agrees with the experimental data (2.83°). Conversely, the calculated angle for **4c** (26.33°) slightly deviates from the corresponding experimental data (16.78°). The discrepancy between the calculation results and experimental data may have been caused by intermolecular interactions in the latter. The calculated HOMOs and LUMOs of all of the compounds are shown in Figures 4,

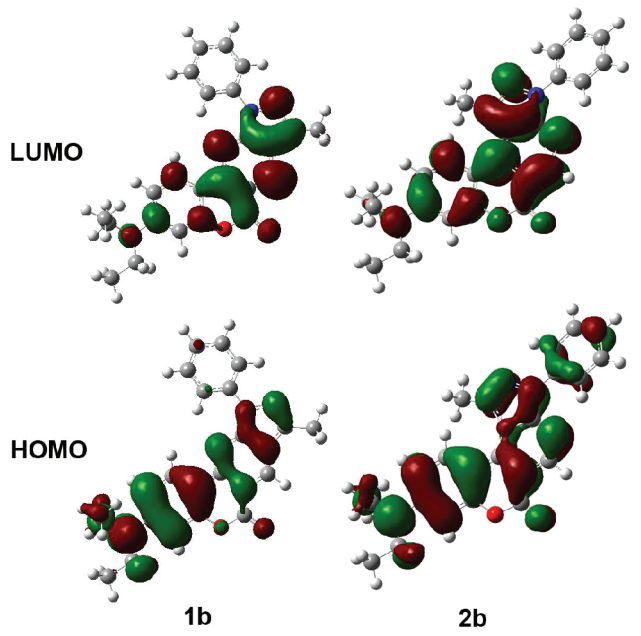

Figure 4. Spatial distributions of calculated HOMOs and LUMOs of compounds **1b** and **2b**.

S12, and S13. The density of all of the compounds in terms of HOMOs and LUMOs was predominantly localized on the tetracyclic structure. The C−C condensation products **1a**−**1d** exhibited stronger ICT character and effective electronic communication between the diethylamino group and pyrazolopyridine core. This result was previously confirmed by the photophysical properties.

Photostability and Cell Imaging. To evaluate the practical utility of the dyes, photostability studies were performed by continuous irradiation of **1a** and **2a** (compared with coumarin 151) using a 500 W high-pressure mercury lamp

dx.doi.org/10.1021/jo3002722 | J. Org. Chem. 2012, 77, 3475−3482

as the light source. Photoinduced bleaching was quantified by monitoring absorption intensity as a function of irradiation time (Figure 5). Compound **1a** exhibited greater photostability than

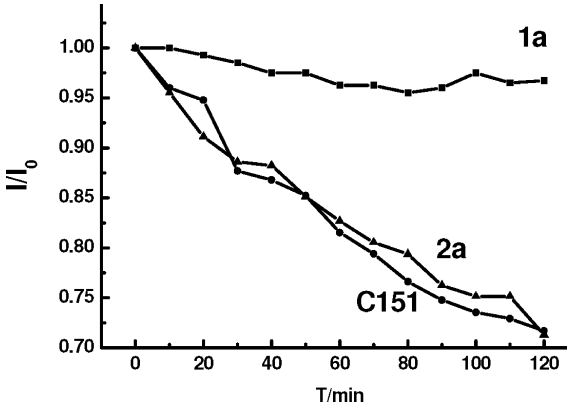

Figure 5. Photostability of compounds **1a**, **2a**, and coumarin 151 in ethanol. Absorption intensity was measured at 373 nm for **1a**, at 403 nm for **2a**, and at 381 nm for coumarin 151.

2a and commercial dye coumarin 151. After 2 h of continuous ultraviolet irradiation, the absorbance of **1a** remained stable, whereas that of **2a** dropped by 28.7%, which was comparable to that of coumarin 151 (28.3%). We tested **1a** and **2a** for bioimaging in HeLa cells. As shown in Figure 6, intense

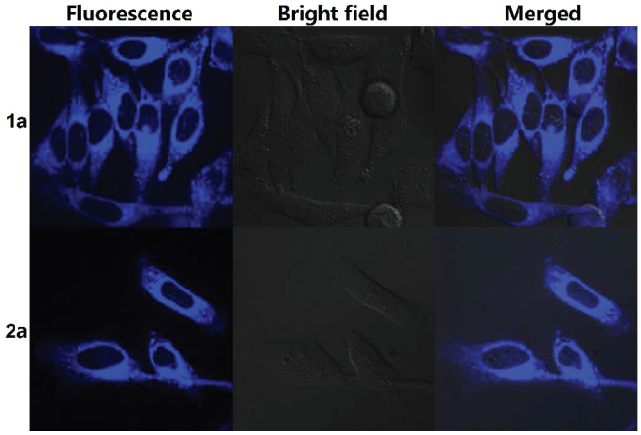

Figure 6. Confocal fluorescence images of living HeLa cells with **1a** (10 μM) and **2a** (50 nM).

intracellular blue fluorescence was observed in the cytosol of HeLa cells after being incubated with dyes **1a** (10 μM) and **2a** (50 nM) for 20 min. The high fluorescence quantum yields were sufficient for highly fluorescent cell staining for only 50 nM for dye **2a**. The blue fluorescence of **1a** may have originated from the aggregation of the dye, as evidenced by the corresponding emission spectra of **1a** in aqueous ethanol with different ethanol/water ratios. Figure S14 illustrates that increasing water content in ethanol caused the peak of emission spectra to move from 572 to 480 nm. This result is consistent with fluorescence in the solid state (479 nm). The above-mentioned results reveal that the tetracyclic PPC derivatives **1a** and **2a** can efficiently penetrate the cell membrane and specifically label cytosol.

CONCLUSIONS

In this study, we developed a one-pot synthesis approach to the construction of two different pyrazolo[3,4-*b*]pyridine-based coumarin molecular skeleton, which showed high fluorescence quantum yields in both less polar solvents and the solid state with ICT character. The relationships between the chemical structures and properties of these compounds were investigated by X-ray diffraction, absorption spectroscopy, fluorescence spectroscopy, single photon counting technique, cyclic voltammetry, thermogravimetric analysis, and DFT calculations. This work provides a promising strategy for exploiting pyrazolo[3,4-*b*]pyridine-based coumarin derivatives. In addition, laser scanning confocal microscopy experiments confirmed that these compounds can be successfully used in living HeLa cells. Further development of pyrazolo [3,4-*b*]pyridine-based coumarin chromophores in the red part of the spectrum and their applications in organic electroluminescent devices or chemosensors are in progress in our laboratory.

EXPERIMENTAL SECTION

Materials and Methods. All commercial chemicals were used without further purification. Single crystals of compounds **1a**, **1b**, **2b**, and **4a**−**4d** suitable for X-ray crystallographic analysis were obtained by slow diffusion of hexane into ethanol solution of the compounds at ambient temperature. Data collection was done on an MM007-HF CCD (Saturn 724+) diffractometer with Mo Kα radiation (λ = 0.71073 Å) at 173 K. ^{1}H NMR and ^{13}C NMR spectra were recorded at 400 and 100 MHz, respectively. Absorption and fluorescence spectra of all compounds were obtained in a Hitachi U-3010 absorption spectrometer and a Hitachi F-4500 fluorescence spectrometer at 25 °C, respectively. The stock solutions of all compounds were prepared in CH_2Cl_2 (1.0×10^{-3} M). All fluorescence spectra were recorded under 350 nm excitation. Fluorescence quantum yields were measured using coumarin 151 in hexane as the reference (Φ_f = 0.19).[30] All cyclic voltammetry (CV) measurements were recorded in CH_3CN with 0.1 M tetrabutylammonium hexafluorophosphate as supporting electrolyte (scan rate 100 mV/s). The experiments were performed at room temperature with a conventional three-electrode configuration consisting of a glass carbon working electrode, a platinum wire counter electrode, and a nonaqueous Ag/AgCl reference electrode. The working electrode was polished with a 0.05 μm alumina paste and sonicated for 2 min before use. The electrolyte solution was degassed by bubbling with argon for 15 min before measurement. HeLa cells (gifted from the center of cells, Peking Union Medical College) were cultured in confocal dishes in culture media (Dulbecco's modified Eagle medium (DMEM) supplemented with 10% fetal bovine serum (FBS), 50 unit/mL penicillin, and 50 mg/mL of streptomycin) under 5% carbon dioxide/air at 37 °C in a humidified incubator. After 24 h, the cells were incubated with dyes **1a** (10 μM) and **2a** (50 nM) for 20 min. The stock solutions of **1a** (1.0×10^{-3} M) and **2a** (1.0×10^{-5} M) were prepared in CH_2Cl_2. The cells were washed with PBS (phosphate buffered saline) at least five times, and their fluorescence images were taken by confocal fluorescence microscopy.

Synthesis of 3-Aldehyde-7-diethylaminocoumarin (5). Compound **5** was synthesized according to our previously reported work:[12a] ^{1}H NMR (400 MHz, $CDCl_3$) δ 10.13 (s, 1H), 8.26 (s, 1H), 7.43 (d, 1H), 6.67 (d, 1H), 6.50 (s, 1H), 3.49 (m, 4H), 1.25 (t, 6H).

Synthesis of 3-Acetyl-7-diethylaminocoumarin (6). 4-Diethylaminosalicylaldehyde (1.12 g, 5.8 mmol), diethylmalonate (1 mL, 7.9 mmol), and morpholine (0.25 mL) were added into anhydrous ethanol (15 mL). The mixture was refluxed for 2 h, and **6** was obtained by filtration as a yellow solid (1.2 g, 80%): ^{1}H NMR (400 MHz, $CDCl_3$) δ 8.42 (s, 1H), 7.40−7.38 (d, 1H), 6.63−6.60 (q, 1H), 6.47−6.46 (d, 1H), 3.48−3.42 (q, 4H), 2.67 (s, 3H), 1.25−1.22 (t, 6H).

Synthesis of Compounds 1a, 2a, 9, and 10. Compounds **5** (0.5 g, 2.04 mmol) and **7a** (0.39 g, 2.45 mmol) were added into anhydrous ethanol (50 mL). The mixture was refluxed for 8 h. Then the solvent

dx.doi.org/10.1021/jo3002722 | J. Org. Chem. 2012, 77, 3475−3482

was removed under vacuum, and the products were purified by column chromatography using v(EA)/v(petroleum ether, PA) = 1:15 as the eluent.

*9-Diethylamino-2-phenyl-[1]benzopyrano[2,3-e]pyrazolo[3,4-b]-pyridine-6-one (**1a**):* Yellow solid (0.39 g, 50%); mp 224−225 °C; R_f = 0.46 in EA/PA = 1:4; ^{1}H NMR (400 MHz, $CDCl_3$) δ 9.01 (s, 1H), 8.44−8.41 (m, 3H), 8.31 (s, 1H), 7.61−7.57 (m, 2H), 7.39−7.36 (m, 1H), 6.77−6.75 (d, 1H), 6.57 (s, 1H), 3.49−3.44 (q, J = 7.04 Hz, 4H), 1.27−1.24 (t, J = 7.04 Hz, 6H); ^{13}C NMR (100 MHz, $CDCl_3$) δ 162.4, 155.0, 152.2, 152.0, 151.3, 139.4, 136.0, 134.8, 129.2, 126.5, 126.3, 121.1, 116.4, 111.2, 109.3, 107.5, 97.9, 45.0, 12.7; SIMS-HRMS m/z calcd for $[C_{23}H_{20}N_4O_2 + H]^+$ 385.1659, found 385.1658.

*9-Diethylamino-3-phenyl-[1]benzopyrano[4,3-d]pyrazolo[3,4-b]-pyridine-6-one (**2a**):* Yellow solid (0.18 g, 23%); mp 201−202 °C; R_f = 0.29 in EA/PA = 1:4; ^{1}H NMR (400 MHz, $CDCl_3$) δ 9.40 (s, 1H), 8.73 (s, 1H), 8.22−8.20 (m, 3H), 7.59−7.55 (m, 2H), 7.42−7.38 (m, 1H), 6.83−6.80 (m, 1H), 6.63−6.62 (m, 1H), 3.52−3.46 (q, J = 7.12 Hz, 4H), 1.30−1.26 (t, J = 7.12 Hz, 6H); ^{13}C NMR (100 MHz, $CDCl_3$) δ 161.3, 155.8, 152.4, 152.0, 151.5, 139.1, 138.9, 134.7, 129.2, 127.9, 127.1, 122.4, 109.6, 109.1, 108.5, 104.8, 98.3, 45.1, 12.6; SIMS-HRMS m/z calcd for $[C_{23}H_{20}N_4O_2 + H]^+$ 385.1659, found 385.1656.

*3-Bis(5-amino-1-phenylpyrazole-4-yl)methyl-7-diethylaminocoumarin (**9**):* Filemot solid (85 mg, 8%); mp 119−120 °C; R_f = 0.18 in EA/PA = 2:1; ^{1}H NMR (400 MHz, $CDCl_3$) δ 7.61−7.57 (m, 5H), 7.51−7.47 (m, 6H), 7.38−7.34(m, 2H), 7.28−7.26 (m, 1H), 6.61−6.59 (m, 1H), 6.52−6.51 (m, 1H), 5.16 (s, 1H), 3.98 (b, 4H), 3.45−3.39 (q, J = 7.04 Hz, 4H), 1.23−1.19 (t, J = 7.04 Hz, 6H); ^{13}C NMR (100 MHz, $CDCl_3$) δ 163.6, 155.7, 150.4, 142.3, 140.1, 139.6, 138.8, 129.6, 128.9, 127.5, 124.0, 123.1, 109.1, 108.8, 103.7, 97.3, 44.9, 30.5, 12.5; SIMS-HRMS m/z calcd for $[C_{32}H_{31}N_7O_2 + H]^+$ 546.2612, found 546.2619.

*(Z)-7-Diethylamino-3-(1-phenylpyrazole-5-ylimino)-methylcoumarin (**10**):* Red solid (40 mg, 5%); mp 206−208 °C; R_f = 0.49 in EA/PA = 1:2; ^{1}H NMR (400 MHz, $CDCl_3$) δ 8.89 (s, 1H), 8.37 (s, 1H), 7.76−7.74 (m, 2H), 7.65−7.64 (m, 1H), 7.55−7.46 (m, 2H), 7.42−7.33 (m, 2H), 6.63−6.60 (m, 1H), 6.51−6.50 (m, 1H), 6.38−6.37 (m, 1H), 3.47−3.43 (q, J = 7.12 Hz, 4H), 1.27−1.23 (t, J = 7.12 Hz, 6H); ^{13}C NMR (100 MHz, $CDCl_3$) δ 162.2, 157.9, 155.3, 152.4, 150.5, 141.7, 140.3, 139.7, 131.3, 128.6, 126.8, 124.5, 114.7 109.9, 108.9, 97.3, 93.9, 45.2, 12.6; SIMS-HRMS m/z calcd for $[C_{23}H_{22}N_4O_2 + H]^+$ 387.1816, found 387.1821.

Synthesis of Compounds 1b and 2b. Compounds **5** (0.35 g, 1.43 mmol) and **7b** (0.31 g, 1.79 mmol) were added into anhydrous ethanol (40 mL). The mixture was refluxed for 8 h, and **1b** was obtained by filtration. Then the solvent of filtrate was removed under vacuum, and **2b** was purified by column chromatography using v(EA)/v(PA) = 1:15 as the eluent.

*9-Diethylamino-4-methyl-2-phenyl-[1]benzopyrano[2,3-e]-pyrazolo[3,4-b]pyridine-6-one (**1b**):* Yellow solid (0.39 g, 69%); mp 218−220 °C; R_f = 0.43 in EA/PA = 1:4; ^{1}H NMR (400 MHz, $CDCl_3$) δ 8.92 (s, 1H), 8.41−8.38 (m, 3H), 7.58−7.53 (m, 2H), 7.35−7.31 (m, 1H), 6.76−6.74 (d, 1H), 6.56 (s, 1H), 3.49−3.43 (q, J = 7.12 Hz, 4H), 2.67 (s, 3H), 1.27−1.23 (t, J = 7.12 Hz, 6H); ^{13}C NMR (100 MHz, $CDCl_3$) δ 162.6, 155.0, 152.6, 152.1, 150.9, 145.1, 139.4, 134.0, 129.1, 126.5, 125.9, 120.7, 116.7, 110.3, 109.6, 108.0, 98.3, 45.3, 12.6; SIMS-HRMS m/z calcd for $[C_{24}H_{22}N_4O_2 + H]^+$ 399.1816, found 399.1810.

*9-Diethylamino-1-methyl-3-phenyl-[1]benzopyrano[4,3-d]-pyrazolo[3,4-b]pyridine-6-one (**2b**):* Yellow solid (7.2 mg, 1%); mp 211−213 °C; R_f = 0.32 in EA/PA = 1:4; ^{1}H NMR (400 MHz, $CDCl_3$) δ 9.34 (s, 1H), 8.32−8.30 (d, 1H), 8.15−8.13 (m, 2H), 7.56−7.52 (m, 2H), 7.38−7.34 (m, 1H), 6.77−6.74 (m, 1H), 6.62−6.61 (m, 1H), 3.50−3.45 (q, J = 7.08 Hz, 4H), 3.00 (s, 3H), 1.29−1.25 (t, J = 7.08 Hz, 6H); ^{13}C NMR (100 MHz, $CDCl_3$) δ 161.7, 155.7, 153.5, 152.3, 151.0, 143.1, 141.4, 138.7, 130.2, 129.3, 127.0, 122.7, 109.2, 109.0, 108.9, 105.3, 99.0, 45.3, 20.0, 12.6; GCT-MS m/z calcd for $C_{24}H_{22}N_4O_2^+$ 398.1737, found 398.1749.

Synthesis of 9-Diethylamino-2,4-diphenyl-[1]benzopyrano-[2,3-*e*]pyrazolo[3,4-*b*]pyridine-6-one (1c). Compounds **5** (0.22 g, 0.90 mmol) and **7c** (0.28 g, 0.12 mmol) were added into anhydrous ethanol (20 mL). The mixture was refluxed for 8 h, and **1c** was obtained by filtration as a yellow solid (0.31 g, 75%): mp 221−222 °C; R_f = 0.54 in EA/PA = 1:4; ^{1}H NMR (400 MHz, $CDCl_3$) δ 9.25 (s, 1H), 8.52−8.49 (d, 2H), 8.41−8.38 (d, 1H), 8.10−8.08 (d, 2H), 7.61−7.54 (m, 4H), 7.52−7.50 (m, 1H), 7.39−7.35 (m, 1H), 6.76−6.74 (d, 1H), 6.54 (s, 1H), 3.48−3.43 (q, J = 7.08 Hz, 4H), 1.27−1.23 (t, J = 7.04 Hz, 6H); ^{13}C NMR (100 MHz, $CDCl_3$) δ 162.6, 155.0, 153.1, 152.0, 151.3, 146.2, 139.4, 135.2, 131.9, 129.5, 129.2, 129.1, 127.6, 126.5, 126.2, 121.1, 114.7, 111.1, 109.3, 107.4, 97.8, 45.0, 12.7; SIMS-HRMS m/z calcd for $C_{29}H_{24}N_4O_2^+$ 460.1894, found 460.1893.

Synthesis of 9-Diethylamino-2-methyl-4-phenyl-[1]-benzopyrano[2,3-*e*]pyrazolo[3,4-*b*]pyridine-6-one (1d). Compounds **5** (0.22 g, 0.90 mmol) and **7d** (0.18 g, 1.04 mmol) were added into anhydrous ethanol (15 mL). The mixture was refluxed for 8 h, and **1d** was obtained by filtration as a yellow solid (0.27 g, 76%): mp 219−220 °C; R_f = 0.46 in EA/PA = 1:4; ^{1}H NMR (400 MHz, $CDCl_3$) δ 9.24 (s, 1H), 8.47−8.45 (d, 1H), 8.02−8.00 (d, 2H), 7.55−7.52 (m, 2H), 7.48−7.44 (m, 1H), 6.80 (s, 1H), 6.62 (s, 1H), 4.25 (s, 3H), 3.49−3.44 (q, J = 7.04 Hz, 4H), 1.28−1.24 (t, J = 7.04 Hz, 6H); ^{13}C NMR (100 MHz, $CDCl_3$) δ 162.9, 154.8, 153.4, 151.6, 151.2, 144.8, 135.3, 132.3, 129.1, 129.0, 127.1, 126.1, 112.8, 110.5, 109.0, 107.3, 97.7, 44.9, 34.0, 12.6; SIMS-HRMS m/z calcd for $[C_{24}H_{22}N_4O_2 + H]^+$ 399.1816, found 399.1809.

Synthesis of 9-Diethylamino-5-methyl-3-phenyl-[1]-benzopyrano[4,3-*d*]pyrazolo[3,4-*b*]pyridine-6-one (4a). Compounds **6** (1.06 g, 4.09 mmol) and **7a** (0.64 g, 4.03 mmol) were added into anhydrous ethanol (50 mL). The mixture was refluxed for 15 h, and **4a** was obtained by filtration as a yellow solid (0.31 g, 19%): mp 240−241 °C; R_f = 0.39 in EA/PA = 1:4; ^{1}H NMR (400 MHz, $CDCl_3$) δ 8.68 (s, 1H), 8.30−8.28 (m, 2H), 8.23−8.21 (m, 1H), 7.57−7.53 (m, 2H), 7.38−7.35 (m, 1H), 6.81−6.78 (m, 1H), 6.59−6.58 (m, 1H), 3.50−3.45 (q, J = 7.08 Hz, 4H), 3.12 (s, 3H), 1.29−1.25 (t, J = 7.12 Hz, 6H); ^{13}C NMR (100 MHz, $CDCl_3$) δ 164.1, 160.7, 155.6, 151.3, 150.5, 140.8, 139.1, 134.8, 129.1, 128.0, 126.7, 122.0, 109.4, 108.5, 107.6, 105.3, 97.8, 45.0, 28.6, 12.6; SIMS-HRMS m/z calcd for $C_{24}H_{22}N_4O_2^+$ 398.1737, found 398.1742.

Synthesis of 9-Diethylamino-1,5-dimethyl-3-phenyl-[1]-benzopyrano[4,3-*d*]pyrazolo[3,4-*b*]pyridine-6-one (4b). Compounds **6** (110.1 mg, 0.43 mmol) and **7b** (96.2 mg, 0.56 mmol) were added into anhydrous ethanol (15 mL). The mixture was refluxed for 15 h, and **4b** was obtained by filtration as a yellow solid (40 mg, 23%): mp 219−220 °C; R_f = 0.50 in EA/PA = 1:4; ^{1}H NMR (400 MHz, $CDCl_3$) δ 8.26−8.24 (m, 2H), 8.13−8.11 (d, 1H), 7.55−7.51 (m, 2H), 7.35−7.32 (m, 1H), 6.81−6.78 (d, 1H), 6.64−6.63 (m, 1H), 3.51−3.46 (q, J = 7.08 Hz, 4H), 3.09 (s, 3H), 2.90 (s, 3H), 1.29−1.26 (t, J = 7.08 Hz, 6H); ^{13}C NMR (100 MHz, $CDCl_3$) δ 163.5, 160.9, 155.3, 151.9, 150.6, 143.3, 143.0, 139.0, 130.7, 129.1, 126.5, 122.2, 108.9, 108.4, 106.0, 98.6, 45.6, 28.3, 19.4, 12.5; SIMS-HRMS m/z calcd for $C_{25}H_{24}N_4O_2^+$ 412.1894, found 412.1891.

Synthesis of 9-Diethylamino-5-methyl-1,3-diphenyl-[1]-benzopyrano[4,3-*d*]pyrazolo[3,4-*b*]pyridine-6-one (4c). Compounds **6** (418.5 mg, 1.71 mmol) and **7c** (362.5 mg, 1.54 mmol) were added into anhydrous ethanol (15 mL). The mixture was refluxed for 15 h, and **4c** was obtained by filtration as a yellow solid (124 mg, 17%): mp 252−253 °C; R_f = 0.51 in EA/PA = 1:4; ^{1}H NMR (400 MHz, $CDCl_3$) δ 8.36−8.34 (d, 2H), 7.61−7.53 (m, 4H), 7.46−7.42 (m, 3H), 7.38−7.35 (m, 1H), 7.10−7.08 (d, J = 9.16 Hz, 1H), 6.53 (s, 1H), 6.03−6.01 (d, J = 8.88 Hz, 1H), 3.39−3.33 (q, J = 7.08 Hz, 4H), 3.15 (s, 3H), 1.19−1.15 (t, J = 7.08 Hz, 6H); ^{13}C NMR (100 MHz, $CDCl_3$) δ 163.9, 161.0, 155.3, 152.0, 150.9, 147.5, 143.1, 139.1, 134.9, 132.8, 129.7, 129.1, 128.8, 128.6, 126.8, 122.5, 108.6, 107.4, 106.5, 104.3, 97.3, 45.1, 28.3, 12.5; SIMS-HRMS m/z calcd for $C_{30}H_{26}N_4O_2^+$ 474.2050, found 474.2052.

Synthesis of 9-Diethylamino-3,5-dimethyl-1-phenyl-[1]-benzopyrano[4,3-*d*]pyrazolo[3,4-*b*]pyridine-6-one (4d). Compounds **6** (302.5 mg, 1.23 mmol) and **7d** (222.4 mg, 1.29 mmol) were added into anhydrous ethanol (15 mL). The mixture was refluxed for 15 h, and **4d** was obtained by filtration as a yellow solid (107 mg, 22%): mp 220−221 °C; R_f = 0.34 in EA/PA = 1:4; ^{1}H NMR (400 MHz, $CDCl_3$) δ 7.52−7.49 (m, 2H), 7.43−7.40 (m, 3H), 7.08−7.06 (d, J = 9.12 Hz, 1H), 6.48 (s, 1H), 5.99−5.96 (d, J = 9.16 Hz, 1H), 4.24 (s, 3H), 3.37−3.32 (q, J = 7.12 Hz, 4H), 3.13 (s, 3H), 1.18−1.14

dx.doi.org/10.1021/jo3002722 | J. Org. Chem. 2012, 77, 3475−3482

(t, J = 7.08 Hz, 6H); ^{13}C NMR (100 MHz, $CDCl_3$) δ 163.3, 161.2, 155.3, 152.0, 151.0, 146.3, 143.2, 135.2, 132.7, 129.6, 128.6, 107.8, 107.2, 104.8, 104.2, 97.0, 44.9, 34.3, 28.1, 12.6; SIMS-HRMS m/z calcd for $C_{25}H_{24}N_4O_2^+$ 412.1894, found 412.1891.

■ ASSOCIATED CONTENT

Supporting Information

X-ray structure details for **1a**, **1b**, **2b**, **4a**−**4d**, and **9** (CIF); photophysical data; electrochemical data; theoretical calculations and ^{1}H NMR and ^{13}C NMR spectra for new compounds. This material is available free of charge via the Internet at http://pubs.acs.org.

■ AUTHOR INFORMATION

Corresponding Author

*E-mail: wangpf@mail.ipc.ac.cn.

Author Contributions

§J.C. and W.L. contributed equally to this paper.

Notes

The authors declare no competing financial interest.

■ ACKNOWLEDGMENTS

This work is financially supported by the National Natural Science Foundation of China (Grant Nos. 61178061, 20903110), the National High Technology Research and Development Program of China (863 Program) (Grant No. 2011AA03A110), and the Beijing Natural Science Foundation (Grant No. 2111002).

■ REFERENCES

(1) Schmidt, R. D.; Oh, J. H.; Sun, Y.-S.; Deppisch, M.; Krause, A.-M.; Radacki, K.; Braunschweig, H.; Könemann, M.; Erk, P.; Bao, Z.; Würthner, F. *J. Am. Chem. Soc.* **2009**, *131*, 6215.

(2) Karuppannan, S.; Chambron, J. C. *Chem.—Asian J.* **2011**, *6*, 964.

(3) (a) Wang, P. F.; Xie, Z. Y.; Hong, Z. R.; Tang, J. X.; Wong, O. Y.; Lee, C. S.; Wong, N. B.; Lee, S. T. *J. Mater. Chem.* **2003**, *13*, 1894. (b) Wang, P. F.; Xie, Z. Y.; Wong, O. Y.; Lee, C. S.; Wong, N. B.; Hung, L. S.; Lee, S. T. *Chem. Commun.* **2002**, 1404.

(4) (a) Svetlik, J.; Veizerová, L.; Mayer, T. U.; Catarinella, M. *Bioorg. Med. Chem. Lett.* **2010**, *20*, 4073. (b) Chioua, M.; Samadi, A.; Soriano, E.; Lozach, O.; Meijer, L.; Marco-Contelles, J. *Bioorg. Med. Chem. Lett.* **2009**, *19*, 4566.

(5) (a) Mac, M.; Uchacz, T.; Danel, A.; Danel, K.; Kolek, P.; Kulig, E. *J. Fluoresc.* **2011**, *21*, 375. (b) Gondek, E.; Nizioł, J.; Danel, A.; Szlachcic, P.; Pluciński, K.; Sanetra, J.; Kityk, I. V. *Spectrochim. Acta, Part A* **2010**, *75*, 1501. (c) Rurack, K.; Danel, A.; Rotkiewicz, K.; Grabka, D.; Spieles, M.; Rettig, W. *Org. Lett.* **2002**, *4*, 4647.

(6) Tao, Y. T.; Chuen, C. H.; Ko, C. W.; Peng, J. W. *Chem. Mater.* **2002**, *14*, 4256.

(7) (a) Dekic, B. R.; Radulovic, N. S.; Dekic, V. S.; Vukicevic, R. D.; Palic, R. M. *Molecules* **2010**, *15*, 2246. (b) Chia, Y. C.; Chang, F. R.; Wang, J. C.; Wu, C. C.; Chiang, M. Y. N.; Lan, Y. H.; Chen, K. S.; Wu, Y. C. *Molecules* **2008**, *13*, 122. (c) El-Seedi, H. R. *J. Nat. Prod.* **2007**, *70*, 118.

(8) (a) Zhang, H.; Yu, T. Z.; Zhao, Y. L.; Fan, D. W.; Xia, Y. J.; Zhang, P. *Synth. Met.* **2010**, *160*, 1642. (b) Yu, T. Z.; Zhang, P.; Zhao, Y. L.; Zhang, H.; Meng, J.; Fan, D. W.; Chen, L. L.; Qiu, Y. Q. *Org. Electron.* **2010**, *11*, 41. (c) Liu, Z. W.; Helander, M. G.; Wang, Z. B.; Lu, Z. H. *J. Phys. Chem. C* **2010**, *114*, 11931.

(9) (a) Voutsadaki, S.; Tsikalas, G. K.; Klontzas, E.; Froudakis, G. E.; Katerinopoulos, H. E. *Chem. Commun.* **2010**, *46*, 3292. (b) Shao, J. *Dyes Pigm.* **2010**, *87*, 272.

(10) (a) Raikar, U. S.; Tangod, V. B.; Mannopantar, S. R.; Mastiholi, B. M. *Opt. Commun.* **2010**, *283*, 4289. (b) Mannekutla, J. R.; Mulimani, B. G.; Inamdar, S. R. *Spectrochim. Acta, Part A* **2008**, *69*, 419.

(11) Ruiz, M.; Lopez-Alvarado, P.; Giorgi, G.; Menendez, J. C. *Chem. Soc. Rev.* **2011**, *40*, 3445.

(12) (a) Wu, J. S.; Liu, W. M.; Zhuang, X. Q.; Wang, F.; Wang, P. F.; Tao, S. L.; Zhang, X. H.; Wu, S. K.; Lee, S. T. *Org. Lett.* **2006**, *9*, 33. (b) Lee, S.; Sivakumar, K.; Shin, W. S.; Xie, F.; Wang, Q. *Bioorg. Med. Chem. Lett.* **2006**, *16*, 4596.

(13) (a) Chen, T.; Xu, X. P.; Ji, S. J. *J. Comb. Chem.* **2010**, *12*, 659. (b) Chen, H.; Shi, D. Q. *J. Comb. Chem.* **2010**, *12*, 571.

(14) Saiz, C.; Wipf, P.; Mahler, G. *J. Org. Chem.* **2011**, *76*, 5738.

(15) Kleinpeter, E.; Lammermann, A.; Kuhn, H. *Org. Biomol. Chem.* **2011**, *9*, 1098.

(16) Bai, H. T.; Lin, H. C.; Luh, T. Y. *J. Org. Chem.* **2010**, *75*, 4591.

(17) Kolosov, D.; Adamovich, V.; Djurovich, P.; Thompson, M. E.; Adachi, C. *J. Am. Chem. Soc.* **2002**, *124*, 9945.

(18) Machado, A. E. D.; de Miranda, J. A. *J. Photochem. Photobiol., A* **2001**, *141*, 109.

(19) Du, C. Y.; Chen, J. M.; Guo, Y. L.; Lu, K.; Ye, S. H.; Zheng, J.; Liu, Y. Q.; Shuai, Z. G.; Yu, G. *J. Org. Chem.* **2009**, *74*, 7322.

(20) Palsson, L. O.; Wang, C. S.; Batsanov, A. S.; King, S. M.; Beeby, A.; Monkman, A. P.; Bryce, M. R. *Chem.—Eur. J.* **2010**, *16*, 1470.

(21) Moss, K. C.; Bourdakos, K. N.; Bhalla, V.; Kamtekar, K. T.; Bryce, M. R.; Fox, M. A.; Vaughan, H. L.; Dias, F. B.; Monkman, A. P. *J. Org. Chem.* **2010**, *75*, 6771.

(22) Estrada, L. A.; Neckers, D. C. *J. Org. Chem.* **2009**, *74*, 8484.

(23) Shao, J. J.; Guan, Z. P.; Yan, Y. L.; Jiao, C. J.; Xu, Q. H.; Chi, C. Y. *J. Org. Chem.* **2011**, *76*, 780.

(24) Levitus, M.; Zepeda, G.; Dang, H.; Godinez, C.; Khuong, T.-A. V.; Schmieder, K.; Garcia-Garibay, M. A. *J. Org. Chem.* **2001**, *66*, 3188.

(25) Wolak, M. A.; Melinger, J. S.; Lane, P. A.; Palilis, L. C.; Landis, C. A.; Delcamp, J.; Anthony, J. E.; Kafafi, Z. H. *J. Phys. Chem. B* **2006**, *110*, 7928.

(26) Tang, X. L.; Liu, W. M.; Wu, J. S.; Lee, C. S.; You, J. J.; Wang, P. F. *J. Org. Chem.* **2010**, *75*, 7273.

(27) (a) Zhang, Q. M.; Lei, Y. L.; Song, Q. L.; Chen, P.; Zhang, Y.; Xiong, Z. H. *Appl. Phys. Lett.* **2011**, *98*, 243303. (b) Li, N.; Wang, P. F.; Lai, S.-L.; Liu, W. M.; Lee, C. S.; Lee, S. T.; Liu, Z. T. *Adv. Mater.* **2010**, *22*, 527.

(28) (a) Yeh, T. S.; Chow, T. J.; Tsai, S. H.; Chiu, C. W.; Zhao, C. X. *Chem. Mater.* **2006**, *18*, 832. (b) Thomas, K. R. J.; Lin, J. T.; Tao, Y. T.; Chuen, C. H. *Chem. Mater.* **2004**, *16*, 5437.

(29) Frisch, M. J.; Trucks, G. W.; Schlegel, H. B.; Scuseria, G. E.; Robb, M. A.; Cheeseman, J. R.; Montgomery, J. A., Jr.; Vreven, T.; Kudin, K. N.; Burant, J. C.; Millam, J. M.; Iyengar, S. S.; Tomasi, J.; Barone, V.; Mennucci, B.; Cossi, M.; Scalmani, G.; Rega, N.; Petersson, G. A.; Nakatsuji, H.; Hada, M.; Ehara, M.; Toyota, K.; Fukuda, R.; Hasegawa, J.; Ishida, M.; Nakajima, T.; Honda, Y.; Kitao, O.; Nakai, H.; Klene, M.; Li, X.; Knox, J. E.; Hratchian, H. P.; Cross, J. B.; Bakken, V.; Adamo, C.; Jaramillo, J.; Gomperts, R.; Stratmann, R. E.; Yazyev, O.; Austin, A. J.; Cammi, R.; Pomelli, C.; Ochterski, J. W.; Ayala, P. Y.; Morokuma, K.; Voth, G. A.; Salvador, P.; Dannenberg, J. J.; Zakrzewski, V. G.; Dapprich, S.; Daniels, A. D.; Strain, M. C.; Farkas, O.; Malick, D. K.; Rabuck, A. D.; Raghavachari, K.; Foresman, J. B.; Ortiz, J. V.; Cui, Q.; Baboul, A. G.; Clifford, S.; Cioslowski, J.; Stefanov, B. B.; Liu, G.; Liashenko, A.; Piskorz, P.; Komaromi, I.; Martin, R. L.; Fox, D. J.; Keith, T.; Al-Laham, M. A.; Peng, C. Y.; Nanayakkara, A.; Challacombe, M.; Gill, P. M. W.; Johnson, B.; Chen, W.; Wong, M. W.; Gonzalez, C.; Pople, J. A. *Gaussian 03*; Gaussian, Inc.: Wallingford, CT, 2004.

(30) Rechthaler, K.; Kohler, G. *Chem. Phys.* **1994**, *189*, 99.